Applied Catalysis B: Environmental 193 (2016) 226–233

Contents lists available at ScienceDirect

Applied Catalysis B: Environmental

journal homepage: www.elsevier.com/locate/apcatb

Photoactive and metal-free polyamide-based polymers for water and wastewater treatment under visible light irradiation

Junjie Shen[a,*], Roman Steinbach[a], John M. Tobin[a], Mayumi Mouro Nakata[a], Matthew Bower[b], Martin R.S. McCoustra[a], Helen Bridle[a], Valeria Arrighi[a], Filipe Vilela[a,*]

[a] School of Engineering and Physical Sciences, Heriot-Watt University, Edinburgh, EH14 4AS, United Kingdom
[b] Drinking Water Quality Regulator for Scotland, Edinburgh, EH6 6WW, United Kingdom

ARTICLE INFO

Article history:
Received 11 February 2016
Received in revised form 1 April 2016
Accepted 8 April 2016
Available online 11 April 2016

Keywords:
Heterogeneous photosensitizer
Visible light photoactivation
Metal-free polymerization
Singlet oxygen
Water treatment

ABSTRACT

A photoactive benzothiadiazole (BT) based monomer was developed and used in the synthesis of typical polyamide (PA) polymers. The monomer was incorporated in different percentages within the PA backbone of the polymers and their photosensitising ability was tested in different media and conditions. Photochemical experiments in a commercial flow reactor under aerobic conditions showed that the polymers had increased efficiency in singlet oxygen generation compared to the original photoactive monomer. When suspended in aqueous solutions, these materials demonstrated superior photostability towards long-term exposure to light and chemical stability in a wide-range of pH environments. The photoactive polymers were highly capable of degrading two well-known wastewater contaminants, bisphenol A (BPA) and cimetidine, as well as inactivating the waterborne parasite *Cryptosporidium*. Given the simplicity of the synthetic preparation of the polymers, the absence of metals and their photoactivity under visible light, herein we show that these materials are very promising for simultaneous decontamination and disinfection of water.

1. Introduction

When it comes to reducing the impact that we, as a society, have on our environment it is important that water treatment is at the top of our list of priorities. Water is probably our most valuable natural resource and it is absolutely vital to sustain populations, industries and the environment. With a wide range of uses, a comprehensive water management plan can be applied to not only lessen the stress placed on the environment, but also protect public health. Water and wastewater purification is therefore essential to prepare this valuable resource for human use.

Photocatalytic water treatment by singlet oxygen ($^1O_2$) has in recent years gained increasing interest as it involves three environmentally friendly components, namely the photosensitizer, a light source, and molecular oxygen. Common visible light active photosensitizers include organic dyes (*e.g.* Rose Bengal and Methylene Blue), fullerenes, porphyrins, phthalocyanines and transition metal complexes [1–8]. When exposed to light of an appropriate wavelength, the photosensitizer rapidly absorbs energy and is electronically excited to its triplet state through an intersystem crossing mechanism, the excited photosensitizer is then capable of transferring energy to the ground state triplet oxygen to form the reactive $^1O_2$ [9].

$^1O_2$ is a selective oxidant which readily oxidizes unsaturated double bonds, phenols, sulfides, amines and other electron-donor compounds due to its electrophilic nature [9]. $^1O_2$ is also highly cytotoxic and is thus capable of killing cells and microorganisms [10,11]. With regard to water and wastewater treatment, $^1O_2$ becomes particularly attractive because it can carry out dual function of decontamination and disinfection [12]. Unlike conventional technologies which in most cases merely separate contaminants from water, $^1O_2$ can convert organic contaminants into biodegradable compounds as well as kill bacteria, fungi, and viruses [9,13,14]. Meanwhile, $^1O_2$ is much more selective towards organic compounds compared to the hydroxyl radical ($OH^\bullet$) and other nonspecific oxidants [15]. The selectivity of $^1O_2$ enhances its oxidation capacity when target pollutants are present in complex wastewater matrices with background constituents (*e.g.* natural

Abbreviations: ABT, 4,4-(benzo[c][1,2,5]thiadiazole-4,7-diyl)dianiline; BBT, 4,7-bis(4,4,5,5-tetramethyl-1,3,2-dioxaborolan-2-yl)benzo[c][1,2,5]thiadiazole; BPA, bisphenol A; BT, Benzothiadiazole; FFA, furfuryl alcohol; MPD, *m*-phenylendiamine; PA, polyamide; PA-ABT (x%), ABT incorporated polyamide; PBS, phosphate-buffered saline; $Pd(PPh_3)_4$, tetrakis(triphenylphosphine)palladium; TMC, trimesoylchloride.

* Corresponding authors.
E-mail addresses: js315@hw.ac.uk (J. Shen), f.vilela@hw.ac.uk (F. Vilela).

http://dx.doi.org/10.1016/j.apcatb.2016.04.015
0926-3373/

organic matter). Recent research showed that $^1O_2$ was more efficient than non-selective OH• in removal of some pharmaceuticals in real wastewater effluents [13].

Although photosensitized $^1O_2$ has numerous advantages, there are a few limitations. (i) Many organic photosensitizers incorporate diverse metal species with visible light harvesting capacity [16–19]. These organic-metal complexes tend to be expensive, toxic and unsustainable [20]; (ii) the vast majority of photosensitizers work in homogeneous conditions. When employing a homogeneous photosensitizer in water its separation and recovery becomes a severe problem and there is an increased risk of leakage of the photosensitizer which may lead to environmental pollution [21]; (iii) some photosensitizers suffer from photobleaching, which refers to the degradation of the photosensitizer *via* long exposure to light and/or to the generated $^1O_2$ [9]. Photobleaching significantly reduces the quantum yield and the lifetime of the photosensitizer. It is therefore desirable to develop heterogeneous and metal-free photosensitizers, which are photostable towards light and $^1O_2$.

Immobilizing the photosensitizer onto a solid support allows it to be easily recovered and reused [9]. Many common photosensitizers, such as Rose Bengal, 5,10,15,20-tetrakis(*p*-hydroxyphenyl)porphyrin, and C_{60} aminofullerene, have been immobilized on different solid supports, including silica nanoparticles [22], silica gels [23], chitosan [24], and some hydrophilic polymers [25]. Immobilization can also increase the photostability because the matrix constitutes an efficient oxygen diffusion barrier that inhibits photobleaching [26]. For the same reason, the quantum yield and thus the photocatalysis efficiency of the photosensitizer might be reduced after immobilization [9]. Nevertheless the benefits of having a heterogeneous and stable photosensitising system outweigh the lower photocatalysis efficiencies.

Herein we report on the synthesis and characterization of a conjugated photosensitizer and its incorporation into a series of polymers. Benzothiadiazole (BT) is a strong electron-accepting moiety due to its small electronic band-gap and high absorption coefficient [27]. The combination of BT with weak electron-donors increases the yield of intersystem crossing to the triplet state, leading to the formation of an efficient photosensitizer [27]. In this work, the photosensitizer was introduced into a polyamide backbone *via* a metal-free step-growth strategy to ensure that the catalytic activity was not induced by the presence of any metal contaminant. The resulting photoactive materials, amphiphilic in nature, show enhanced $^1O_2$ production when simply using air as the source of oxygen, in both organic and aqueous media under visible light irradiation.

2. Experimental

2.1. Synthesis of $^1O_2$ photosensitizer and incorporation into polyamide matrix

The photosensitizer monomer is an aminophenyl-substituted benzothidiazole derivative and is here abbreviated as ABT. It was synthesized through Suzuki-Miyaura cross-coupling of 4-bromoaniline with 4,7-bis(4,4,5,5-tetramethyl-1,3,2-dioxaborolan-2-yl)benzo[c][1,2,5]thiadiazole (BBT) in the presence of $Pd(PPh_3)_4$ and a base (Scheme 1).

The photoactive polymers were prepared *via* the metal-free polymerization reaction between ABT, *m*-phenylendiamine (MPD), and trimesoylchloride (TMC) (Scheme 2). This method is based on the MPD-TMC reaction described by Ghosh, et al. [28]. Similar to MPD, ABT contains diamine groups and can thus undergo polymerization reaction with TMC. By replacing a selected amount of MPD in the polymerization reaction, the photosensitizer monomer ABT was introduced into PA backbone. The mole ratio of (MPD + ABT) to TMC in the polymerization reaction was fixed at 1.45. For each polymerization reaction, the product was named as PA-ABT (x%). The number x% indicates the molar percent of ABT in (MPD + ABT). It is noted that this number might not reflect the final concentration of ABT in the resultant PA-ABT (x%). Specific quantities of ABT and MPD are provided in the Supplementary material (Table S1). Given that PA-ABT (x%) are thermoset polymers with cross-linked structure, it is difficult to determine the exact amount of ABT incorporated. Instead, the relative abundance of ABT in different PA-ABT (x%) polymers was evaluated by FT-IR, and the resulting photoactivity of the derived materials in the production of $^1O_2$ increased with the increase of the ABT monomer fed into the polymerization as detailed in the following sections.

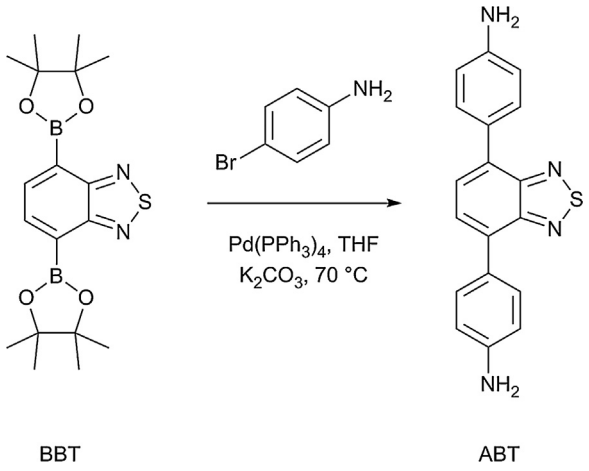

Scheme 1. Synthetic scheme of the photosensitizer monomer.

2.2. Photosensitized $^1O_2$ production and contaminant degradation

The photochemical experiments were conducted in a commercial flow reactor (Easy-Photochem system from Vapourtec, Ltd.) (Fig. 1). Compared to conventional batch systems this offers consistent light penetrations and controlled exposure times, which leads to more efficient $^1O_2$ generation. Certain amount of ABT monomer or PA-ABT (x%) was added into a 20 mL solution containing a target substrate (α-terpinene, FFA, BPA or cimetidine). For $^1O_2$ production in chloroform, 500 mg/L ABT monomer or PA-ABT (x%) was added into 0.1 M α-terpinene solution. For $^1O_2$ production in water, 50 mg/L PA-ABT (25%) was added into 0.1 mM FFA/BPA/cimetidine solution. The mixture was pumped into the tubing and mixed with air from separate tubing using a T-junction. The mixture was in this way pumped into the flow reactor equipped with a 420 nm LED lamp, and recirculated several times through the reactor itself. The flow rates of solution and air were fixed at 2 mL/min and 1 mL/min, respectively. The reactor was maintained at room temperature without heating or cooling, with negligible heating observed from the LED module. Sample aliquots of 1 mL were collected at constant time intervals for further analysis. FFA conversion by PA-ABT (25%) was repeated over five cycles in order to test the photostability of the polymers. After one cycle of photochemical reaction, PA-ABT (25%) was separated through centrifugation and washed with water before being used in the next cycle. Negative control experiments were performed using the same procedure in the absence of photosensitizer or light, or oxygen.

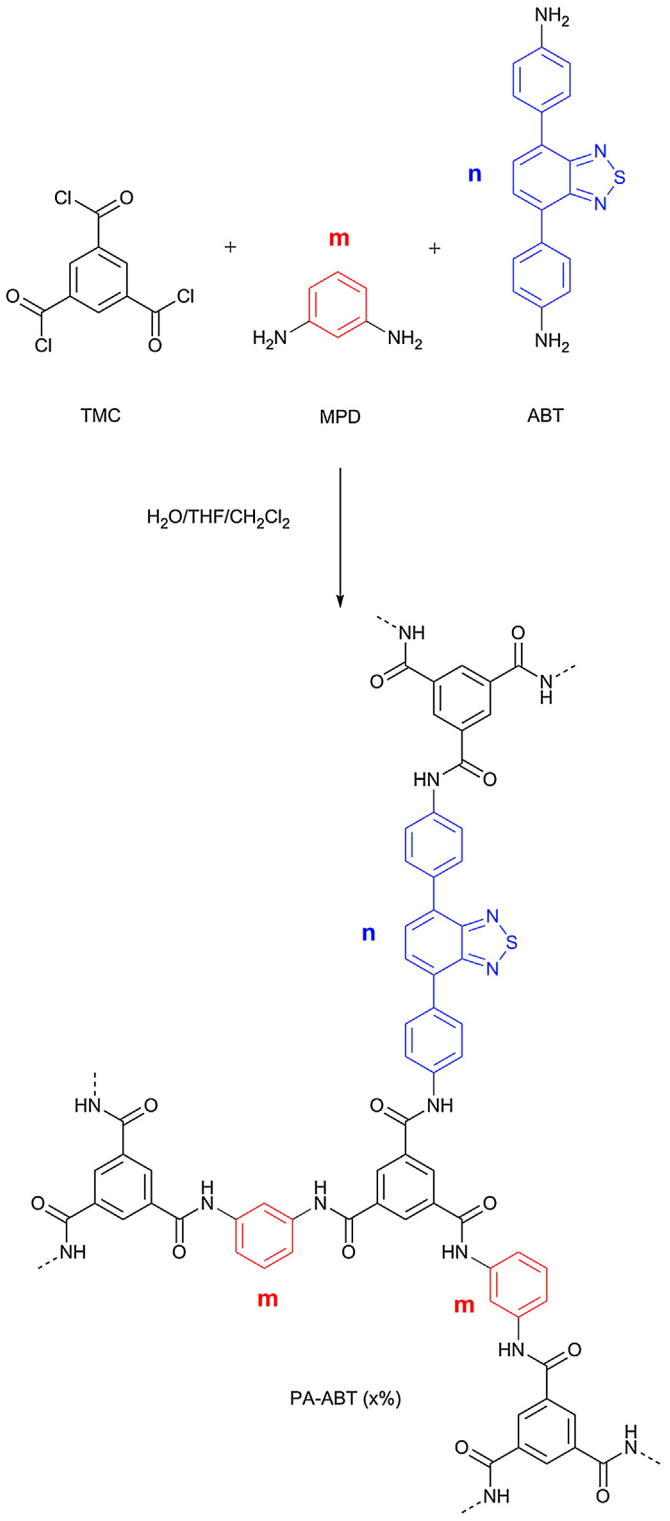

Scheme 2. Synthetic scheme for the photoactive polymer and representation of a possible fragment of the polymer network.

2.3. *Photocatalytic inactivation of* Cryptosporidium

The disinfection capacity of PA-ABT (25%) was assessed through a *Cryptosporidium* inactivation experiment. Four samples were prepared and each sample contained 1 million oocysts in 200 μL PBS solution (Table 4). Samples 1 and 2 had no PA-ABT (25%) while Samples 3 and 4 each contained 50 mg/L PA-ABT (25%). Samples 2 and 4 were exposed to visible light at 420 nm wavelength for

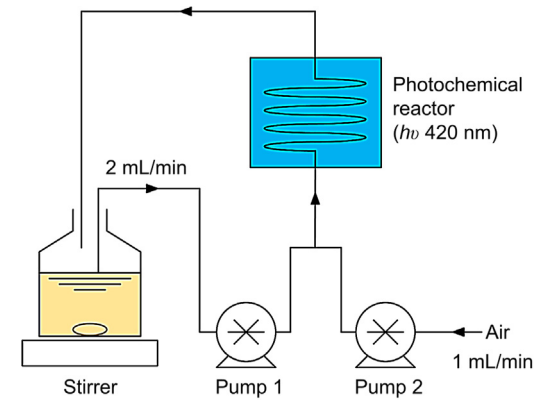

Fig. 1. Schematic representation of the Vapourtec Ltd. flow reactor.

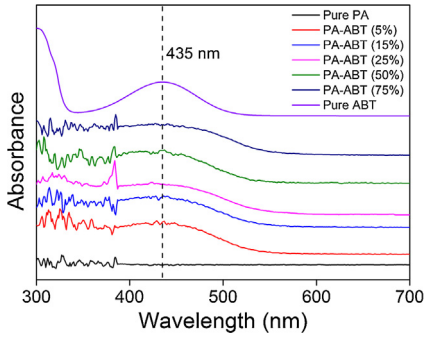

Fig. 2. UV/Vis spectra of pure ABT, PA-ABT (x%) and pure PA.

one hour (selected as a feasible disinfection time and using previous organic contaminant degradation data as a starting point). To ensure adequate oxygen mixing, the samples were vortexed every 10 min. The excystation assay to determine the impact upon viability was developed by Blewett [29]. Viability of *Cryptosporidium* was assessed by counting the number of oocysts, sporozoites and number of empty shells by phase contrast microscopy, expressing the number of empty shells divided by number of oocysts and empty shells as a percentage and thus, a measure of excystation of the parasites. The exact details of the procedure are included in the Supplementary material.

3. Results & discussion

3.1. *Characterization of ABT and PA-ABT (x%)*

The ABT monomer was obtained as a light orange powder while the polymers were yellow powders. The UV/Vis absorption spectrum (Fig. 2) of ABT shows a broad absorption band between 350 and 500 nm with maximum at 435 nm (Soret band), which is assigned to the transition from the electron-donating moiety to the electron-accepting BT moiety [30]. This absorption band was scarcely shifted after ABT was incorporated into polyamide, indicating that no electronic interactions occur between the ABT and TMC monomers. The pure PA, on the other hand, had no adsorption peak at 435 nm.

Fig. 3 presents the FT-IR spectra of pure ABT, PA-ABT (x%) and pure PA. Peaks at 1470–1520 cm^{-1} and 1517–1618 cm^{-1} were observed in all samples, and were attributed to C=C stretching of the aromatic rings and to N—H bending of the amide group, respectively. The peaks at 1658 cm^{-1} that appeared in PA and PA-ABT (x%) but not in ABT monomer were attributed to C=O stretching of amide group. On the other hand, the peaks at 824 cm^{-1} and 892 cm^{-1} were the characteristic peaks for the BT moiety, as they

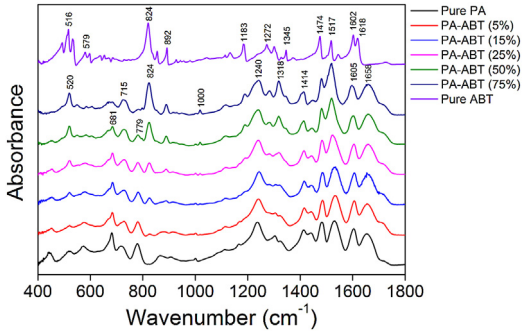

Fig. 3. FT-IR spectra of pure ABT, PA-ABT (x%) and pure PA.

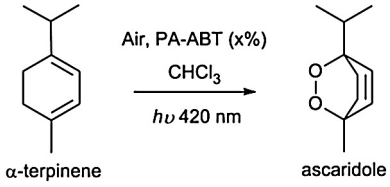

Scheme 3. Conversion of α-terpinene to ascaridole in chloroform.

were observed for ABT and PA-ABT (x%) but not for pure PA. The intensity of the BT peaks increased with increasing amount of ABT in PA-ABT (x%), which indicates the successful incorporation of ABT monomer within the PA backbone. ^{1}H NMR and ^{13}C NMR spectra of ABT monomer and solid state ^{13}C NMR of PA-ABT (25%) are included in the Supplementary material (Figs. S1–S3).

3.2. Photosensitized $^{1}O_2$ production in chloroform

The photoactivity of ABT monomer and PA-ABT (x%) polymers as $^{1}O_2$ photosensitizers was initially tested by employing the conversion of α-terpinene to ascaridole in chloroform (Scheme 3). It is well-known that α-terpinene is extremely susceptible to photosensitized $^{1}O_2$ oxidation whilst being rather stable against other oxygen-rich oxidants such as OH•, ozone (O_3), and hydrogen peroxide (H_2O_2) [31,32]. Ascaridole is the only product and the concentrations of both α-terpinene and ascaridole were measured by ^{1}H NMR (Fig. S4). Chloroform was chosen as the solvent due to the fact that the lifetime of $^{1}O_2$ in chloroform (~250 μs) is considerably longer than its lifetime in water (~2 μs) [33–35].

When irradiated with blue light at 420 nm, ABT monomer and PA-ABT (x%) polymers were able to convert α-terpinene into ascaridole to different extents, whereas the pure PA had no effect on α-terpinene (Fig. 4). This confirms that the conversion of α-terpinene is due to the photochemical generation of $^{1}O_2$. The photochemical reaction between $^{1}O_2$ and the substrate is essentially a second-order reaction, which means the rate of the reaction depends on the concentrations of both reactants. However, in practice, most studies conducted the photochemical reactions in a batch mode where the concentration of the substrate was much greater than the concentration of $^{1}O_2$. Therefore the kinetics of reactions between $^{1}O_2$ and the substrate can be simplified by the pseudo-first-order model [13,14,23]. The pseudo-first-order model is expressed as Eq. (1):

$$-\frac{dC}{dt} = kC \quad (1)$$

where C is the concentration of substrate (mM or mg/L), t is the reaction time (h), and k is the pseudo-first-order rate constant

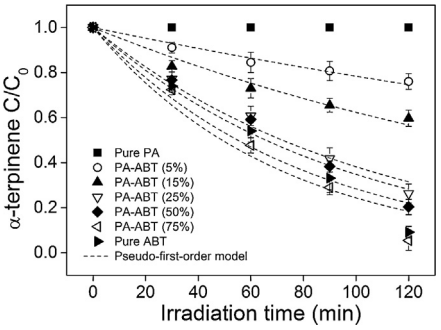

Fig. 4. Conversion of α-terpinene to ascaridole by pure ABT, PA-ABT (x%) and pure PA in chloroform under visible light irradiation as a function of ABT content. Curves represent non-linear regression fits to the pseudo-first-order model. Error bars indicate the standard deviation of three replicate measurements (λ = 420 nm, 0.1 M α-terpinene, 500 mg/L pure ABT/PA-ABT (x%)/pure PA).

Table 1
Pseudo-first-order kinetics parameters of α-terpinene conversion by PA-ABT (x%) and ABT monomer (0.1 M α-terpinene, 500 mg/L ABT monomer or PA-ABT (x%)).

Photosensitizer	k (h^{-1})	R^2
PA-ABT (5%)	0.146	0.974
PA-ABT (15%)	0.284	0.970
PA-ABT (25%)	0.578	0.984
PA-ABT (50%)	0.634	0.971
PA-ABT (75%)	0.848	0.956
Pure ABT	0.756	0.950

Table 2
Pseudo-first-order kinetics parameters of FFA conversion by PA-ABT (25%) (0.1 mM FFA, 50 mg/L PA-ABT (25%), pH 7).

Run	k (h^{-1})	R^2
1	0.144	0.999
2	0.139	0.999
3	0.137	0.999
4	0.136	0.999
5	0.135	0.999

Table 3
Pseudo-first-order kinetics parameters of BPA and cimetidine conversion by PA-ABT (25%) (0.1 mM BPA/cimetidine, 50 mg/L PA-ABT (25%), pH 7).

Condition	k (h^{-1})	R^2
BPA w PA-ABT (25%)	0.562	0.998
BPA w/o PA-ABT (25%)	0.026	0.972
Cimetidine w PA-ABT (25%)	1.297	0.981
Cimetidine w/o PA-ABT (25%)	0.048	0.962

(h^{-1}). If the initial concentration of substrate is C_0, Eq. (1) can be integrated as follow:

$$\ln C - \ln C_0 = -kt \quad (2)$$

Eq. (2) can be further presented in exponential form as follow:

$$\frac{C}{C_0} = e^{-kt} \quad (3)$$

The kinetics of α-terpinene conversion were fitted to the pseudo-first-order model by non-linear regression of concentration *versus* time data (Fig. 4) and the pseudo-first-order rate constants k and correlation coefficients R^2 were determined (Table 1). Results show that the conversion of α-terpinene generally followed the pseudo-first-order model. However, the actual conversion at later stage of the reaction (*e.g.* after 120 min) was considerably higher than the expected conversion based on the pseudo-first-order model. This is probably due to the fact that a continuous flow of air (and hence oxygen) was supplied into

Table 4
Inactivation of *Cryptosporidium* with and without PA-ABT (25%).

Sample	Description	Excystation (%)
1	Live control	90
2	Light only	82
3	PA-ABT (25%) only	80
4	Light + PA-ABT (25%)	65

the flow reactor, which led to continuous $^1O_2$ generation. At later stage of the photochemical reaction, increased concentration of $^1O_2$ and decreased concentration of α-terpinene did not fulfil the condition for the pseudo-first-order model any more. Therefore the actual conversion was higher than that estimated by the pseudo-first-order model. This result highlights a major advantage of the continuous-flow reaction over the batch reaction.

It should be noted that the actual amount of photosensitized $^1O_2$ includes (i) $^1O_2$ interacting with the substrate, (ii) $^1O_2$ quenched by the substrate without reaction and (iii) $^1O_2$ decaying in solution [36]. Given that α-terpinene is not a physical quencher and it has a reaction rate much greater than the natural decay rate of $^1O_2$ in chloroform [36], the generation of $^1O_2$ was inferred from the conversion of α-terpinene into ascaridole. As shown in Fig. 4, the conversion of α-terpinene increased with increasing percentage of ABT in PA-ABT (x%). This is expected since greater amount of ABT generates more $^1O_2$ reactive species. A noticeable result is that PA-ABT (75%) had a comparable α-terpinene conversion to the ABT monomer. This is somewhat surprising given that the mass of ABT in PA-ABT (75%) is much lower than the mass of ABT monomer. Furthermore, ABT monomer acts as a homogenous photosensitizer whereas PA-ABT (x%) polymers produce $^1O_2$ in a heterogeneous fashion. These results suggest that immobilization within the PA network improves the efficacy of ABT in $^1O_2$ generation. Previously, Lee, et al. [23] reported that immobilization of C_{60} aminofullerene on silica support accelerated $^1O_2$ production. They attributed the improved photocatalysis efficiency to decreased C_{60} aggregation in aqueous solution [23]. This was not the case here since ABT was soluble in chloroform and dispersible in water [37]. However, the major disadvantage of employing the ABT monomer as a photosensitizer on its own is that it suffers from photobleaching, which means that ABT monomer either decomposes in the given conditions or it may react with the $^1O_2$ once formed. A colour change from light yellow to dark brown was observed in the ABT solution during the photochemical reaction (Fig. S5). On the other hand, PA-ABT (x%) did not experience photobleaching owing to the highly cross-linked character of the polymeric backbone. The improved photostability by immobilization enables long-term use of ABT without significant loss of activity, leading to an enhanced $^1O_2$ production. In control experiments, negligible conversion of α-terpinene occurred in the absence of ABT or PA-ABT (x%) under light; in the presence of ABT or PA-ABT (x%) under light in a N_2-saturated environment; and in the presence of ABT or PA-ABT (x%) in dark. Negative control experiments verify that the photosensitizer, light and O_2 are the three essential elements for initiating a photochemical reaction.

3.3. Photosensitized $^1O_2$ production in water

PA-ABT (25%) was selected for subsequent experiments because it achieved comparatively high conversion of α-terpinene at relatively moderate ABT content. Experiments in aqueous solutions were carried out to test the suitability of PA-ABT (25%) for water treatment. FFA, which is water soluble and does not quench the excited states of various sensitizers, was used as the $^1O_2$ specific substrate in water. It has been reported that the influence of other oxidants such as $OH^•$ and H_2O_2 on FFA is insignificant [38]. The

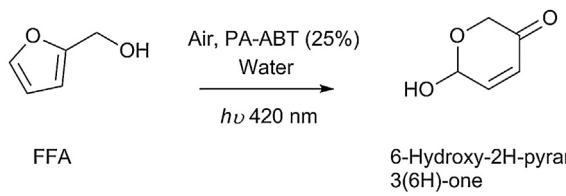

Scheme 4. Conversion of FFA to 6-hydroxy-2H-pyran-3(6H)-one in water.

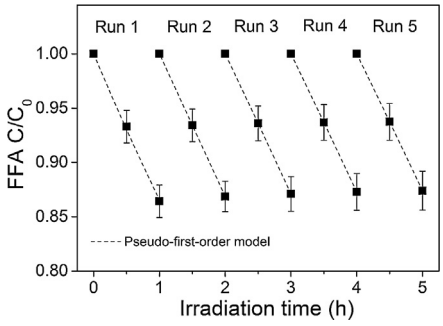

Fig. 5. Repeated conversion of FFA by PA-ABT (25%) in water under visible light irradiation. Curves represent non-linear regression fits to the pseudo-first-order model. Error bars indicate the standard deviation of three replicate measurements (λ = 420 nm, 0.1 mM FFA, 50 mg/L PA-ABT (25%), pH 7).

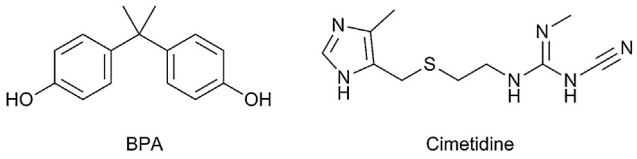

Scheme 5. Structure of BPA and cimetidine.

major reaction products of FFA and $^1O_2$ are 6-hydroxy-2H-pyran-3(6H)-one and H_2O_2, with the produced H_2O_2 having negligible effect on the reaction [38] (Scheme 4). The $^1O_2$ production was measured *via* the consumption of FFA using HPLC (Fig. S6).

Fig. 5 shows that approximately 14% of FFA was converted within the first 1 h by PA-ABT (25%). The reaction was stopped after 1 h. The photosensitizer polymer was recovered from the suspension by centrifugation and reused for another 1 h experiment run, treating the same amount of FFA as the initial run. In total, the process was repeated 5 times using the same polymer. As can be seen from Fig. 5 and Table 2, the conversion of FFA by PA-ABT (25%) fits the pseudo-first-order model very well. Despite loss of PA-ABT (25%) during centrifugation, the reduction in conversion of FFA over the 5 repeated runs was small, which implies good photostability of PA-ABT (25%) as a photosensitizer. In the future, when used in a larger amount, the photosensitizer polymer can be more completely recovered from suspension by advanced separation techniques such as membrane filtration and solid phase extraction.

3.4. Degradation of emerging contaminants

Two emerging contaminants, BPA and cimetidine, were selected as typical wastewater contaminants to be treated by the photocatalytic polymer [39] (Scheme 5). BPA is widely used as a monomer for making polycarbonate plastic and epoxy resins. It exhibits hormone-disrupting properties and has been shown to cause negative health effects in animal studies [40]. Cimetidine is a pharmaceutical compound used in the treatment of heartburn and peptic ulcers. It poses an environmental threat due to its physiological effect on humans [41]. These two contaminants

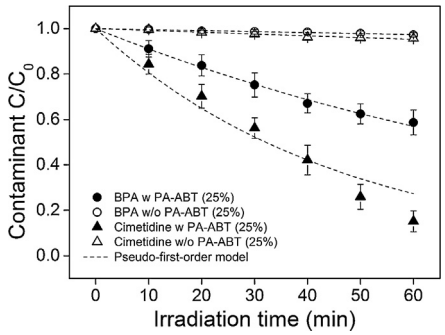

Fig. 6. Conversion of BPA and cimetidine by PA-ABT (25%) in water under visible light irradiation. Curves represent non-linear regression fits to the pseudo-first-order model. Error bars indicate the standard deviation of three replicate measurements (λ = 420 nm, 0.1 mM BPA/cimetidine, 50 mg/L PA-ABT (25%), pH 7).

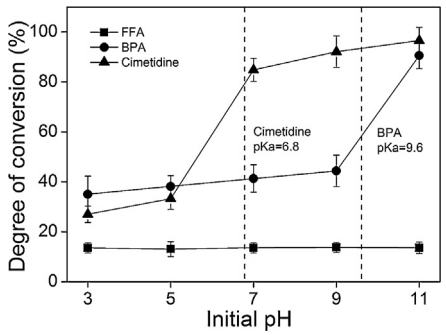

Fig. 7. Conversion of FFA, BPA, and cimetidine by PA-ABT (25%) in water as a function of initial pH under 1 h of visible light irradiation. Error bars indicate the standard deviation of three replicate measurements (λ = 420 nm, 0.1 mM FFA/BPA/cimetidine, 50 mg/L PA-ABT (25%)).

have previously been used as model substrates in photochemical degradation studies, when employing photosensitizers such as TiO_2 [42], C_{60} fullerene [13], and $NaBiO_3$ [14]. The major advantage of using BPA and cimetidine in photochemical reactions is that the degradation mechanisms are well understood.

The concentrations of BPA and cimetidine were quantified by HPLC analysis (Figs. S7 and S8). Based on the HPLC results, PA-ABT (25%) achieved efficient conversion of BPA and cimetidine under visible light of 420 nm (Fig. 6). The conversion of BPA and cimetidine also followed the pseudo-first-order model while some deviations at later stage were due to the excessive amount of $^1O_2$. The degradation pathway for photochemical reaction between BPA and $^1O_2$ has been extensively studied [14,43–45]. On the one hand, $^1O_2$ directly attacks the aromatic ring of BPA, leading to the formation of BPA catechol [44]. On the other hand, $^1O_2$ readily cleaves the bond between two aromatic rings, producing phenol, 4-isopropylphenol, and hydroquinone [14,43,45]. A previous study reported that BPA catechol has a weaker estrogenic activity than BPA [46]. However, future studies are needed to determine and fully understand the estrogenic activity and toxicity of these intermediates under environmental conditions. As for cimetidine, Latch, et al. [41] investigated its degradation pathway by using model compounds. They found that the imidazole model compound reacted 12 times faster with $^1O_2$ than the sulphide model system and 500 times faster than the cyanoguanidine model compound, indicating that the imidazole ring is the dominant reactive group [41]. The interaction of imidazole derivatives with $^1O_2$ leads to the formation of endoperoxides which eventually decompose to form CO_2 [47].

Direct photolysis experiments showed minor degradation of BPA and cimetidine in the first 60 min. The photostability of these compounds can be rationalized by the fact that they lack chromophores capable of absorbing light at 420 nm wavelength (UV/Vis spectra in Fig. S9). It is worth mentioning that BPA and cimetidine both undergo spontaneous photochemical reactions upon irradiation in the presence of dissolved organic matter, which absorbs light and produces $^1O_2$ and other reactive oxygen species [41,48]. No direct dark transformation of BPA and cimetidine occurred in the presence of PA-ABT (25%) alone.

3.5. Effect of pH on photocatalytic performance

Since the pH of wastewater may vary significantly depending on the source and environment, PA-ABT (25%) was further tested under different pH conditions. The photocatalytic performance of PA-ABT (25%) was quantified by the degree of conversion of substrate. The degree of conversion was defined as the concentration reduction after 1 h photochemical reaction:

$$\text{degree of conversion} = \frac{C_0 - C_{1h}}{C_0} \times 100\% \quad (4)$$

where C_0 and C_{1h} are the initial concentration and the concentration after 1 h reaction, respectively.

Fig. 7 shows the degree of conversion of FFA, BPA and cimetidine by PA-ABT (25%) as a function of initial pH. The degree of conversion of FFA was constant (~13.5%) despite of pH variation. It has been shown that the reaction of FFA with $^1O_2$ is independent of pH in the range 5–12 [49]. Therefore, the constant FFA conversion reported here over a wider pH range demonstrates superior chemical stability of PA-ABT (25%). This is promising for water and wastewater treatment because it means the pH can be adjusted to control the speciation of target contaminants without losing the functionality of the photosensitizer. As a result the treatability of water and wastewater that contain pH-dependent contaminants can be maximized.

Both BPA and cimetidine showed pH-dependent degradation by PA-ABT (25%). The degree of conversion of BPA increased from 35% to 44% at pH below 9, and rose steeply to 90% at pH 11 (Fig. 7). This is consistent with the pKa of BPA which was reported to be between 9.6 and 10.2 [50]. At pH > pKa, BPA became negatively charged by the deprotonation of phenol to the phenolate anion. The phenolate anion was more electrophilic than the neutral phenol and reacted more readily with photosensitized $^1O_2$. This leads to a drastic enhancement in the degree of conversion of BPA under alkaline pH [15,43].

Similarly, the pH dependence of cimetidine conversion can be explained considering its pKa which varies from 6.8 to 7 [41]. As shown in Fig. 7, the degree of conversion varied from 27% at pH 3, where cimetidine was primarily in its protonated form, to 96% at pH 11, where the unprotonated cimetidine dominated the speciation. Given that imidazole is the reactive site, the unprotonated imidazole ring has increased electron density and is thus more reactive towards $^1O_2$ [41]. Complete conversion of BPA and cimetidine by PA-ABT (25%) could be obtained at pH values above their pKa. These studies ultimately demonstrate that the photoactive polymer is functioning at a wide range of pH values.

3.6. Disinfection capacity

Cryptosporidium is a protozoan parasite found in soil, food and water that has been contaminated with animal or human faeces. *Cryptosporidium* is of significant public health concern in drinking water because it causes a disease called cryptosporidiosis. Cryptosporidiosis can last up to three weeks in relatively healthy patients but can also be fatal for immunosuppressed individuals

[51]. The traditional chlorination method is unable to remove *Cryptosporidium* from water because *Cryptosporidium* is highly resistant towards chlorine and chloramines, which makes it tougher to kill than most disease-causing pathogens [52,53].

Results of the excystation assay showed that exposure of *Cryptosporidium* to PA-ABT (25%) in combination with visible light irradiation at 420 nm caused a substantial reduction in viability. Excystation percentage decreased from 90% to 65% (Table 4). However, exposure to either PA-ABT (25%) or 420 nm irradiation alone each caused a reduction in viability to an excystation percentage of around 80%. This indicates that the inactivated polymer (in the absence of light) might have potential intrinsic acute toxicity. The detailed mechanism is still unknown.

To the best of our knowledge, this is the first example of protozoan disinfection using a photoactive polymer and is particularly interesting given the resistance of this protozoan parasite to chlorine disinfection. The degree of inactivation observed appears comparable to lower dosages of UV irradiation [54,55]. Greater levels of inactivation can potentially be achieved by longer exposure times and/or higher doses of the photosensitizer. In this study one hour was selected as this timeframe had previously been shown to be effective for organic contaminants and also would be feasible timescale for a disinfection process for this parasite in water treatment. In future work, it would be of interest to further investigate the effect of reaction time and polymer concentrations on excystation rate of *Cryptosporidium*. This would enable identification of optimised water treatment conditions. The effectiveness of the photoactive polymer on bacteria (*e.g. Escherichia Coli*) and virus will also be explored in future work.

4. Conclusions

A series of novel photoactive metal-free polymers PA-ABT (x%) was synthesized by incorporating a photosensitizer monomer ABT into a polyamide structure. Photochemical experiments were conducted in a commercial flow reactor with continuous air injection and visible light illumination. The conversion of α-terpinene to ascaridole in chloroform was used to compare the efficiency of the ABT monomer to that of heterogeneous polymers with varying ABT content. Interestingly, PA-ABT (75%) had a comparable α-terpinene conversion to the ABT monomer, suggesting that immobilization within the PA network improves the efficacy of ABT in $^1O_2$ generation. Kinetic study reveals that in general the photochemical reaction between $^1O_2$ and α-terpinene in chloroform followed the pseudo-first-order model. However, constant injection of air in the flow reactor led to a higher-than-expected α-terpinene conversion at later stage.

PA-ABT (25%) was used in aqueous solution experiments to assess the feasibility of PA-ABT in water and wastewater treatment. Repeated photochemical experiments using FFA as the $^1O_2$ specific substrate in water demonstrated the photostability of PA-ABT (25%). Despite its relatively low photosensitizer content and short exposure time to light, PA-ABT (25%) showed high efficiency in degradation of BPA and cimetidine, and inactivation of *Cryptosporidium*. The photochemical reaction between $^1O_2$ and FFA/BPA/cimetidine in water also followed the pseudo-first-order model. The water pH had no effect on the $^1O_2$ production of PA-ABT (25%), but affected the conversion of pH-dependent contaminants by PA-ABT (25%). This study is the first example of photoactive polymers being applied in the concomitant decontamination and disinfection of water, though further studies on the toxicity of degradation products of various contaminants are required.

PA-ABT (x%) polymers offer several advantages compared to conventional photocatalysts. Firstly, the metal-free synthesis is cost-effective and eco-friendly. Secondly, they function readily under visible light, eliminating the requirement for UV irradiation. Thirdly, their cross-linked structure enhances the photostability and enables easy separation from water. Therefore, these new materials are very suitable candidates in the use of water and wastewater treatment. A natural progression of this work is to develop photoactive polymeric membranes using these materials. Design of associated photocatalytic membrane reactors for pilot-scale applications is also recommended.

Acknowledgements

Filipe Vilela acknowledges Heriot-Watt University and The Royal Society for financial support (RG2014 R2). Vapourtec Ltd. is thanked for their invaluable technical support. The PhD studentship for Junjie Shen was provided by Energy Technology Partnership (ETP) Scholarship with Drinking Water Quality Regulator for Scotland (DWQR) as the industrial sponsor.

Appendix A. Supplementary data

Supplementary data associated with this article can be found, in the online version, at http://dx.doi.org/10.1016/j.apcatb.2016.04.015.

References

[1] T. Hamano, K. Okuda, T. Mashino, M. Hirobe, K. Arakane, A. Ryu, S. Mashiko, T. Nagano, Singlet oxygen production from fullerene derivatives: effect of sequential functionalization of the fullerene core, Chem. Commun. (1997) 21–22.
[2] K. Arakane, A. Ryu, C. Hayashi, T. Masunaga, K. Shinmoto, S. Mashiko, T. Nagano, M. Hirobe, Singlet oxygen (1(g) generation from Coproporphyrin in Propionibacterium acneson irradiation, Biochem. Biophys. Res. Commun. 223 (1996) 578–582.
[3] R. Bonnett, Photosensitizers of the porphyrin and phthalocyanine series for photodynamic therapy, Chem. Soc. Rev. 24 (1995) 19–33.
[4] J.J.M. Lamberts, D.C. Neckers, Rose Bengal derivatives as singlet oxygen sensitizers, Tetrahedron 41 (1985) 2183–2190.
[5] C.K. Prier, D.A. Rankic, D.W.C. MacMillan, Visible light photoredox catalysis with transition metal complexes: applications in organic synthesis, Chem. Rev. 113 (2013) 5322–5363.
[6] R.E. Galian, J. Perez-Prieto, Catalytic processes activated by light, Energy Environ. Sci. 3 (2010) 1488–1498.
[7] L. Villén, F. Manjón, D. García-Fresnadillo, G. Orellana, Solar water disinfection by photocatalytic singlet oxygen production in heterogeneous medium, Appl. Catal. B 69 (2006) 1–9.
[8] P. Krystynik, P. Kluson, S. Hejda, D. Buzek, P. Masin, D.N. Tito, Semi-pilot scale environment friendly photocatalytic degradation of 4-chlorophenol with singlet oxygen species—direct comparison with H_2O_2/UV-C reaction system, Appl. Catal. B 160–161 (2014) 506–513.
[9] M.C. DeRosa, R.J. Crutchley, Photosensitized singlet oxygen and its applications, Coord. Chem. Rev. 233–234 (2002) 351–371.
[10] L.J. Schiff, W.C. Eisenberg, J. Dziuba, K. Taylor, S.J. Moore, Cytotoxic effects of singlet oxygen, Environ. Health Perspect. 76 (1987) 199–203.
[11] M.D. Hernandez-Alonso, F. Fresno, S. Suarez, J.M. Coronado, Development of alternative photocatalysts to TiO_2: challenges and opportunities, Energy Environ. Sci. 2 (2009) 1231–1257.
[12] M. Thandu, C. Comuzzi, D. Goi, Phototreatment of water by organic photosensitizers and comparison with inorganic semiconductors, Int. J. Photoenergy 2015 (2015) 22.
[13] H. Kim, W. Kim, Y. Mackeyev, G.-S. Lee, H.-J. Kim, T. Tachikawa, S. Hong, S. Lee, J. Kim, L.J. Wilson, T. Majima, P.J.J. Alvarez, W. Choi, J. Lee, Selective oxidative degradation of organic pollutants by singlet oxygen-mediated photosensitization: tin porphyrin versus C60 aminofullerene systems, Environ. Sci. Technol. 46 (2012) 9606–9613.
[14] T. Zhang, Y. Ding, H. Tang, Generation of singlet oxygen over Bi(V)/Bi(III) composite and its use for oxidative degradation of organic pollutants, Chem. Eng. J. 264 (2015) 681–689.
[15] J. Lee, S. Hong, Y. Mackeyev, C. Lee, E. Chung, L.J. Wilson, J.-H. Kim, P.J.J. Alvarez, Photosensitized oxidation of emerging organic pollutants by tetrakis C_{60} aminofullerene-derivatized silica under visible light irradiation, Environ. Sci. Technol. 45 (2011) 10598–10604.
[16] W.B. Connick, H.B. Gray, Photooxidation of platinum(II) diimine dithiolates, J. Am. Chem. Soc. 119 (1997) 11620–11627.
[17] A.A. Abdel-Shafi, P.D. Beer, R.J. Mortimer, F. Wilkinson, Photosensitized generation of singlet oxygen from ruthenium(II)-substituted benzoaza-crown-bipyridine complexes, Phys. Chem. Chem. Phys. 2 (2000) 3137–3144.

[18] A.A. Abdel-Shafi, P.D. Beer, R.J. Mortimer, F. Wilkinson, Photosensitized generation of singlet oxygen from vinyl linked benzo-crown-ether-bipyridyl ruthenium (II) complexes, J. Phys. Chem. A 104 (2000) 192–202.
[19] A. Goethals, T. Mugadza, Y. Arslanoglu, R. Zugle, E. Antunes, S.W. Hulle, T. Nyokong, K. Clerck, Polyamide nanofiber membranes functionalized with zinc phthalocyanines, J. Appl. Polym. Sci. 131 (2014).
[20] S. Gazi, R. Ananthakrishnan, Metal-free-photocatalytic reduction of 4-nitrophenol by resin-supported dye under the visible irradiation, Appl. Catal. B 105 (2011) 317–325.
[21] T. Nyokong, V. Ahsen, Photosensitizers in Medicine, Environment, and Security, Springer, Netherlands, 2012.
[22] G. Yanyan, R. Snezna, Z. Peng, Rose Bengal-decorated silica nanoparticles as photosensitizers for inactivation of gram-positive bacteria, Nanotechnology 21 (2010) 065102.
[23] J. Lee, Y. Mackeyev, M. Cho, L.J. Wilson, J.-H. Kim, P.J.J. Alvarez, C_{60} amino-fullerene immobilized on silica as a visible-light-activated photocatalyst, Environ. Sci. Technol. 44 (2010) 9488–9495.
[24] R. Bonnett, M.A. Krysteva, I.G. Lalov, S.V. Artarsky, Water disinfection using photosensitizers immobilized on chitosan, Water Res. 40 (2006) 1269–1275.
[25] A.P. Schaap, A.L. Thayer, K.A. Zaklika, P.C. Valenti, Photooxygenations in aqueous solution with a hydrophilic polymer-immobilized photosensitizer, J. Am. Chem. Soc. 101 (1979) 4016–4017.
[26] R. Carpentier, R.M. Leblanc, M. Mimeault, Photoinhibition and chlorophyll photobleaching in immobilized thylakoid membranes, Enzyme Microb. Technol. 9 (1987) 489–493.
[27] K. Zhang, D. Kopetzki, P.H. Seeberger, M. Antonietti, F. Vilela, Surface area control and photocatalytic activity of conjugated microporous poly(benzothiadiazole) networks, Angew. Chem. Int. Ed. 52 (2013) 1432–1436.
[28] A.K. Ghosh, B.-H. Jeong, X. Huang, E.M.V. Hoek, Impacts of reaction and curing conditions on polyamide composite reverse osmosis membrane properties, J. Membr. Sci. 311 (2008) 34–45.
[29] D.A. Blewett, Quantitative techniques in *Cryptosporidium* research, in: K.W. Angus, D.A. Blewett (Eds.), Cryptosporidiosis: Proceedings of the 1st International Workshop, Moredun Research Institute, UK, 1989, pp. 85–95.
[30] T. Kato, M. Matsumoto, H. Shigeiwa, S. Gorohmaru, T. Ishi-i, S. Mataka, Novel 2,1,3-benzothiadiazole-based red-fluorescent dyes with enhanced two-photon absorption cross-sections, Chem. Eur. J. 12 (2006) 2303–2317.
[31] S. Ogawa, S. Fukui, Y. Hanasaki, K. Asano, H. Uegaki, F. Sumiko, S. Ryosuke, Determination method of singlet oxygen in the atmosphere by use of α-terpinene, Chemosphere 22 (1991) 1211–1225.
[32] D. Choi, M. Jung, Protective activities of catechins on singlet oxygen induced photooxidation of α-terpinene in methanol: structure and singlet oxygen quenching activity relationship, Food Sci. Biotechnol. 22 (2013) 249–256.
[33] K.I. Salokhiddinov, I.M. Byteva, G.P. Gurinovich, Lifetime of singlet oxygen in various solvents, J. Appl. Spectrosc. 34 (1981) 561–564.
[34] R. Schmidt, Influence of heavy atoms on the deactivation of singlet oxygen (1. DELTA.g) in solution, J. Am. Chem. Soc. 111 (1989) 6983–6987.
[35] F. Wilkinson, W.P. Helman, A.B. Ross, Rate constants for the decay and reactions of the lowest electronically excited singlet state of molecular oxygen in solution—an expanded and revised compilation, J. Phys. Chem. Ref. Data 24 (1995) 663–677.
[36] F. Wilkinson, J.G. Brummer, Rate constants for the decay and reactions of the lowest electronically excited singlet state of molecular oxygen in solution, J. Phys. Chem. Ref. Data 10 (1981) 809–999.
[37] H. Urakami, K. Zhang, F. Vilela, Modification of conjugated microporous polybenzothiadiazole for photosensitized singlet oxygen generation in water, Chem. Commun. 49 (2013) 2353–2355.
[38] W.R. Haag, J. Hoigne, E. Gassman, A.M. Braun, Singlet oxygen in surface waters—Part I: furfuryl alcohol as a trapping agent, Chemosphere 13 (1984) 631–640.
[39] B. Petrie, R. Barden, B. Kasprzyk-Hordern, A review on emerging contaminants in wastewaters and the environment: current knowledge, understudied areas and recommendations for future monitoring, Water Res. 72 (2015) 3–27.
[40] L.N. Vandenberg, S. Ehrlich, S.M. Belcher, N. Ben-Jonathan, D.C. Dolinoy, E.R. Hugo, P.A. Hunt, R.R. Newbold, B.S. Rubin, K.S. Saili, A.M. Soto, H.-S. Wang, F.S. vom Saal, Low dose effects of bisphenol A, Endocr. Disruptors 1 (2013) 1–20.
[41] D.E. Latch, B.L. Stender, J.L. Packer, W.A. Arnold, K. McNeill, Photochemical fate of pharmaceuticals in the environment: cimetidine and ranitidine, Environ. Sci. Technol. 37 (2003) 3342–3350.
[42] Y. Ohko, I. Ando, C. Niwa, T. Tatsuma, T. Yamamura, T. Nakashima, Y. Kubota, A. Fujishima, Degradation of bisphenol A in water by TiO_2 photocatalyst, Environ. Sci. Technol. 35 (2001) 2365–2368.
[43] C. Tai, G. Jiang, J. Liu, Q. Zhou, J. Liu, Rapid degradation of bisphenol A using air as the oxidant catalyzed by polynuclear phthalocyanine complexes under visible light irradiation, J. Photochem. Photobiol. A Chem. 172 (2005) 275–282.
[44] Y. Barbieri, W.A. Massad, D.J. Díaz, J. Sanz, F. Amat-Guerri, N.A. García, Photodegradation of bisphenol A and related compounds under natural-like conditions in the presence of riboflavin: kinetics, mechanism and photoproducts, Chemosphere 73 (2008) 564–571.
[45] E. Díez-Mato, F.C. Cortezón-Tamarit, S. Bogialli, D. García-Fresnadillo, M.D. Marazuela, Phototransformation of model micropollutants in water samples by photocatalytic singlet oxygen production in heterogeneous medium, Appl. Catal. B 160–161 (2014) 445–455.
[46] X. Ye, X. Zhou, L. Needham, A. Calafat, In-vitro oxidation of bisphenol A: is bisphenol A catechol a suitable biomarker for human exposure to bisphenol A? Anal. Bioanal. Chem. 399 (2011) 1071–1079.
[47] P. Kang, C.S. Foote, Photosensitized oxidation of ^{13}C, ^{15}N-labeled imidazole derivatives, J. Am. Chem. Soc. 124 (2002) 9629–9638.
[48] Y.-P. Chin, P.L. Miller, L. Zeng, K. Cawley, L.K. Weavers, Photosensitized degradation of bisphenol A by dissolved organic matter, Environ. Sci. Technol. 38 (2004) 5888–5894.
[49] P.G. Tratnyek, J. Hoigne, Oxidation of substituted phenols in the environment: a QSAR analysis of rate constants for reaction with singlet oxygen, Environ. Sci. Technol. 25 (1991) 1596–1604.
[50] C.A. Staples, P.B. Dome, G.M. Klecka, S.T. Oblock, L.R. Harris, A review of the environmental fate, effects, and exposures of bisphenol A, Chemosphere 36 (1998) 2149–2173.
[51] P.R. Hunter, G. Nichols, Epidemiology and clinical features of cryptosporidium infection in immunocompromised patients, Clin. Microbiol. Rev. 15 (2002) 145–154.
[52] D. Korich, J. Mead, M. Madore, N. Sinclair, C.R. Sterling, Effects of ozone chlorine dioxide, chlorine, and monochloramine on *Cryptosporidium parvum* oocyst viability, Appl. Environ. Microbiol. 56 (1990) 1423–1428.
[53] O.K. Dalrymple, E. Stefanakos, M.A. Trotz, D.Y. Goswami, A review of the mechanisms and modeling of photocatalytic disinfection, Appl. Catal. B 98 (2010) 27–38.
[54] G.F. Cotruvo, Providing Safe Drinking Water in Small Systems: Technology, Operations, and Economics, CRC Press, USA, 1999.
[55] United States Environmental Protection Agency, Inactivation of *Cryptosporidium parvum* oocysts in Drinking Water, United States Environmental Protection Agency, USA, 1999.